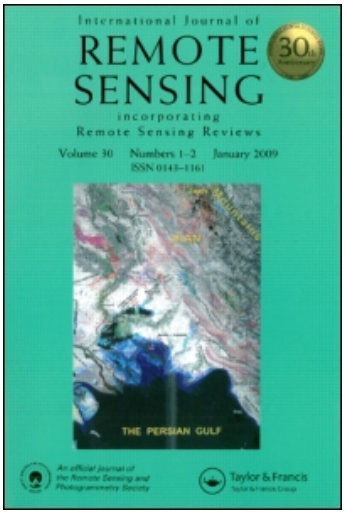

International Journal of Remote Sensing
Publication details, including instructions for authors and subscription information:
http://www.informaworld.com/smpp/title~content=t713722504

Effects of atmospheric water and surface wind on passive microwave retrievals of sea ice concentration: a simulation study

Dong-Bin Shin[a]; Long S. Chiu[b]; Pablo Clemente-Colon[c]
[a] Department of Atmospheric Sciences, Yonsei University, Seoul, Korea [b] Center for Earth Observing and Space Research, George Mason University, Fairfax, USA [c] National Ice Center, Washington, DC 20395, USA

To cite this Article Shin, Dong-Bin , Chiu, Long S. and Clemente-Colon, Pablo(2008) 'Effects of atmospheric water and surface wind on passive microwave retrievals of sea ice concentration: a simulation study', International Journal of Remote Sensing, 29: 19, 5717 — 5731
To link to this Article: DOI: 10.1080/01431160801978999
URL: http://dx.doi.org/10.1080/01431160801978999

International Journal of Remote Sensing
Vol. 29, No. 19, 10 October 2008, 5717–5731

Effects of atmospheric water and surface wind on passive microwave retrievals of sea ice concentration: a simulation study

DONG-BIN SHIN*†, LONG S. CHIU‡ and PABLO CLEMENTE-COLON§
†Department of Atmospheric Sciences, Yonsei University, Seoul, Korea
‡Center for Earth Observing and Space Research, George Mason University, Fairfax, VA 22030, USA
§National Ice Center, Washington, DC 20395, USA

(*Received 30 January 2007; in final form 21 November 2007*)

The atmospheric effects on the retrieval of sea ice concentration from passive microwave sensors were examined using simulated data typical for the Arctic summer. The simulation includes atmospheric contributions of cloud liquid water (CLW), water vapour (WV) and surface wind on the microwave signatures. A plane parallel radiative transfer model was used to compute brightness temperatures at SSM/I frequencies over surfaces that contained open water, first-year (FY) ice, multi-year (MY) ice and their combinations. Synthetic retrievals were performed using the NASA Team (NT) algorithm for the estimation of sea ice concentrations. Our results show that if the satellite sensor's field of view is filled with only FY ice, the retrieval is hardly affected by the atmospheric conditions because of the high contrast between emission signals from the FY ice surface and the atmosphere. Pure MY ice concentration is generally underestimated because of the low MY ice surface emissivity, which results in the enhancement of emission signals from the atmosphere. In marginal ice areas, the atmospheric and surface effects tend to degrade the accuracy at low sea ice concentrations. FY ice concentration is overestimated and MY ice concentration is underestimated in the presence of atmospheric water and surface wind at low ice concentration. Moreover, strong surface wind appears to be more important than atmospheric water in contributing to the retrieval errors of total ice concentrations over marginal ice zones.

1. Introduction

Sea ice has an important role to play in the global climate system. As an insulator, it controls the ocean–atmosphere exchanges of heat, mass, momentum and chemical constituents. Due to its high albedo, it reduces the amount of solar radiation absorbed at the Earth's surface, thus contributing to the 'albedo-temperature' feedback mechanism of the Earth's climate. Oceanic convection is also affected by the change in water density resulting from the release of salt during the ice formation process and the input of fresh water when the ice melts (Gloersen *et al.* 1992). Monitoring sea ice concentration is therefore crucial for early detection of global climate changes. In fact, a reduction in the Arctic sea ice, inferred from satellite observations, has been reported by several investigators (e.g. Johannessen *et al.* 1999, Parkinson *et al.* 1999, Meier *et al.* 2005).

*Corresponding author. Email: dbshin@yonsei.ac.kr

International Journal of Remote Sensing
ISSN 0143-1161 print/ISSN 1366-5901 online
http://www.tandf.co.uk/journals
DOI: 10.1080/01431160801978999

Remote sensing techniques are the most viable approach to monitoring global sea ice concentrations and their changes. However, uncertainties due to sampling, differences in sensor characteristics, surface types (ice, water and snow) and weather interference still pose a major challenge for ice change detection (Meier *et al.* 2004). For example, visible and infrared techniques provide high-resolution retrievals but their capability is restricted to non-cloudy situations and daylight conditions (visible). Microwave radiometry provides almost all-weather monitoring but its low spatial resolution limit its application to large-scale monitoring. Active microwave monitoring by synthetic aperture radar provides detailed monitoring capabilities even under cloudy conditions but the high acquisition costs prohibit its use in routine monitoring. The whole suite of remote sensors is needed for a comprehensive assessment of sea ice conditions.

A series of satellite-borne passive microwave sensors has been deployed or planned for monitoring sea ice conditions. These sensors include the Electrically Scanning Microwave Radiometer onboard the NIMBUS-5 satellite (ESMR-5), the Scanning Multichannel Microwave Radiometer (SMMR) flown on the Nimbus-7 satellite (1978 to 1987), the Special Sensor Microwave/Imagers (SSM/I) on the Defense Meteorological Satellite Program (DMSP) satellites (1987 to present), and the Advanced Microwave Scanning Radiometer onboard NASA's Aqua satellite (AMSR-E). Passive microwave retrievals of sea ice concentration, such as the Norsex (Svendsen *et al.* 1983) and the NASA Team (NT) algorithm (Cavalieri *et al.* 1984), are mostly based on the distinct difference of surface emissivities of ice-free water and the two major types of sea ice: first-year (FY) and multi-year (MY) ices. However, uncertainties such as atmospheric effects, variability of the surface emissivity, especially for MY ice and over marginal ice areas, and the existence of other ice types such as thin ice, melting ice and snow-covered surface contribute to the algorithm uncertainty.

Comparison studies of passive microwave sea ice concentration retrievals such as those by Markus and Dokken (2002) and Anderson *et al.* (2007) have been performed. The atmospheric effects on sea ice retrievals have also been studied by several investigators (e.g. Maslanik 1992, Oelke 1997) based on radiative transfer calculations using the observed radiosonde profile data. Maslanik (1992) and Oelke (1997) show that atmospheric water affects the retrieval of FY and MY ice concentration differently; atmospheric water gives rise to overestimates of FY ice concentrations and underestimates of MY ice concentrations over marginal ice zones.

An assessment of the error contributions to the retrieval will aid sea ice analysts in the use of these remote sensing products in analysing sea ice conditions. Error estimates are also important for the use of sea ice parameters in diagnostics studies and hypotheses testing of climate change scenarios. In this study we used radiative transfer modelling with atmospheric and sea ice models to understand the algorithm error sources in the microwave retrieval of sea ice concentration. The advantages of such an approach are that individual errors may be examined separately and the validation of algorithms is easily carried out from synthetic retrievals.

2. Simulated data and models

In general, the microwave brightness temperature of a pixel for a non-precipitating atmosphere is dependent on the surface temperature and the surface emissivity and is affected by atmospheric cloud liquid water (CLW) and water vapour (WV). The emissivity of FY ice is distinct from that of open water and MY ice (table 1). The

Table 1. Assumed surface emissivities for two types of ices at 19 GHz horizontal polarization (H) and vertical polarization (V) and 37 GHz vertical polarization channels. The emissivity of open water is computed from the surface variables. Tie points are in parentheses.

Surface types	19 GHz-H	19 GHz-V	37 GH-V
First-year (FY) ice	0.90 (242.6 K)	0.95 (254.8 K)	0.94 (252.1 K)
Multi-year (MY) ice	0.72 (197.8 K)	0.82 (222.5 K)	0.62 (182.1 K)
Open water (no wind)	0.30 (98.0 K)	0.63 (178.2 K)	0.72 (207.7 K)

emissivity of MY ice is non-unique or distributed, as the melting and refreezing processes change the brine and air contents of the MY ice, hence the inclusion of air contents can decrease the emissivity due to volume scattering. The microwave surface emissivity of open water is generally a function of the surface temperature, salinity, and surface roughness.

To investigate the effect of atmospheric and surface variability on the estimation of sea ice concentration over various surface types, non-precipitating atmospheric profiles were generated along with surface variables. The simulated geophysical variables were intended to cover the climatological variability of the Arctic environments for a specific season (summer) as used in Markus and Cavalieri (2000). The surface temperatures of open water and sea ice were set to 271 K and 268 K, respectively. To simulate atmospheric variability, 300 atmospheric profiles of varying CLW and WV were generated. The columnar CLW ranges from 0 to $0.3\,\mathrm{kg\,m^{-2}}$ and the columnar WV varies from 1.5 to 8.1 mm at 271 K and from 1.2 to 6.4 mm at 268 K, with a lapse rate of $6\,\mathrm{K\,km^{-1}}$. The surface wind speed (WS) is in the range 0–34 $\mathrm{m\,s^{-1}}$ and the simulations were performed at $2\,\mathrm{m\,s^{-1}}$ intervals (18 WS intervals). These atmospheric parameter ranges are comparable to those used by Mitnik and Mitnik (2004) in the development of atmospheric retrieval algorithms over sea ice (CLW$<0.25\,\mathrm{kg\,m^{-2}}$ and precipitable water of 0.63–18.5 $\mathrm{kg\,m^{-2}}$ in the Okhotsk Sea).

Each wind speed was applied to a set of CLW and WV profiles giving 5400 data sets (300 profiles $\times$ 18 wind speeds = 5400). CLW is distributed with height in the cloudy atmosphere. Cloud heights of 1–5 km were used.

The microwave signatures from these profiles on top of three surface types (open water, FY ice and MY ice) and their combinations were computed. For simplicity, the calculations were performed for sea ice concentrations of 0, 10, 20, 40, 60, 80, 90, 95, and 100%. The simulated data can be used for testing various sea ice algorithms. The NT algorithm (Cavalieri *et al.* 1984) with weather filter was chosen for the current study. Microwave brightness temperatures (T_B) at the frequencies of the SSM/I were computed using a one-dimensional plane parallel Eddington model (Kummerow 1993). The SSM/I has four frequency channels: 19.35, 37.0 and 85.5 GHz with both horizontal and vertical polarizations and 22.24 GHz with only vertical polarization. It views the atmosphere at an earth incidence angle of 53.1°. The fields of view (FOVs) are 70×45, 60×40, 38×30 and $16 \times 14\,\mathrm{km^2}$ at 19.35, 37.0, 22.24 and 85.5 GHz, respectively.

The surface emissivities of FY and MY ice used and the tie points are shown in table 1. These emissivities values are slightly adjusted to approximate the tie points used in the NT sea ice algorithm for the Northern Hemisphere (Comiso *et al.* 1997). The tie points of these surfaces are defined by the T_B observed through a relatively cloud-free (for open water) and calm sea surface (for 100% ice cover). The emissivity for a given incidence angle and polarization was determined by the Fresnel relations

(Jackson 1962). In particular, surface wind roughens the open sea surface and hence the surface emissivity.

In this study, we used the Wilheit (1979) model for wind-roughened sea surface emissivity. In the Wilheit model the surface emissivity is modelled by a distribution of sea surface slopes as a function of wind speed according to Cox and Munk (1955). The wind-roughened surface is modified by a reduction of the surface reflectivity due to wind-driven foam. In the model, the surface reflectivity (R) affected by wind is estimated from an empirical relationship between the ratio of two polarization measurements (horizontal and vertical polarizations at 37 GHz) and wind speed. Ocean foam is then assumed to appear for wind speed greater than $7\,\mathrm{m\,s^{-1}}$ and the fraction K of the foam is approximated as

$$\begin{aligned} &K = 0 \text{ for } w \leq 7\,\mathrm{m\,s^{-1}} \\ &K = 0.006\left(1 - \mathrm{e}^{-f/f_0}\right)(w-7) \text{ for } w > 7\,\mathrm{m\,s^{-1}} \end{aligned} \tag{1}$$

where w is the wind speed, f is the frequency and $f_0 = 7.5$ GHz. The ocean surface emissivity can thus be written as $\varepsilon = 1 - R(1-K)$.

For comparison, we also present emissivities obtained by the Wentz (1992) model. Wentz's model establishes an empirical relationship for the wind-induced emissivity based on the SeaSat microwave radiometer and scatterometer measurements and corrects for the specular emissivity based on the Fresnel equation with an adjustment for the incidence-angle difference between the SeaSat and SSM/I radiometers. Figure 1 shows the emissivities for the horizontal (H) and vertical (V) polarization T_B at 19 and 37 GHz as a function of wind speed computed from the two models. The Wentz model seems to produce slightly higher emissivities at 19 GHz-V with high wind speed and 19 GHz-H, but slightly lower emissivities at 37 GHz-V and 37 GHz-H with high wind speed. The NT ice-retrieval algorithm uses all three channels (19 GHz-H, -V and 37 GHz-V). Our analyses showed that the use of a specific wind model does not affect the major conclusion of our study. The results from the Wilheit model are presented here.

Following Cavalieri *et al.* (1984), the T_Bs for the sensor's FOV, which consists of three surface types, are obtained from a linear combination of T_Bs at each of the three surfaces:

$$T_\mathrm{B} = T_\mathrm{B\_OW} F_\mathrm{OW} + T_\mathrm{B\_FY} F_\mathrm{FY} + T_\mathrm{B\_MY} F_\mathrm{MY} \tag{2}$$

where the subscripts OW, FY and MY denote three ocean surface types, open water (OW), first-year (FY) ice and multi-year (MY) ice, respectively, and the fractions of each surface are indicated by F_OW, F_FY and F_MY. The sum of the fractions is unity.

3. Radiometric signatures of the atmospheric parameters

Two spectral quantities, the polarization ratio (PR) and the spectral gradient ratio (GR), are used in the NT sea ice algorithm. They are defined as follows:

$$\mathrm{PR} = (T_\mathrm{B\_19V} - T_\mathrm{B\_19H})/(T_\mathrm{B\_19V} + T_\mathrm{B\_19H}) \tag{3}$$

$$\mathrm{GR} = (T_\mathrm{B\_37V} - T_\mathrm{B\_19V})/(T_\mathrm{B\_37V} + T_\mathrm{B\_19V}) \tag{4}$$

where the subscripts V and H indicate vertical and horizontal polarizations, respectively.

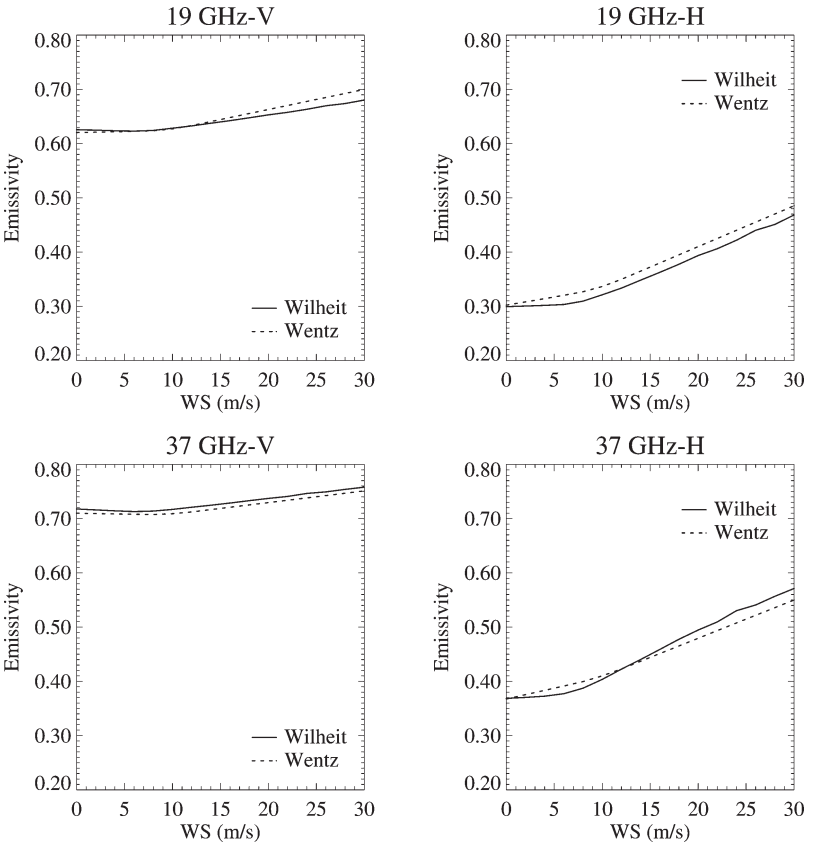

Figure 1. Emissivity of the ocean surface as a function of surface wind speed (WS) for the four SSM/I channels according to the Wilheit (1979) and Wentz (1992) models.

Figure 2 shows the variations in PR and GR as a function of columnar CLW content and columnar WV content. PR (solid line) decreases over both ice types and open water areas as sea ice concentration, WV and CLW increase (figures 2(*a*) and 2(*b*)). The ocean surface is highly polarized at 19 GHz whereas the FY and MY ice polarizations are lower. The increased sea ice concentration, CLW and WV tend to depolarize the microwave radiation. The effect of depolarization due to atmospheric WV and CLW is more pronounced over the open ocean than over sea ice. GR (dotted line) decreases with sea ice concentration and increases with CLW for FY ice. GR shows a slight decrease as WV increases. This is due to the larger increase in WV absorption at 19 GHz than at 37 GHz, and is consistent with the results found in Oelke (1997). For MY ice, GR tends to increase as CLW increases and the increase is greater for higher sea ice cover. This is due to the higher surface reflectivity at 37 GHz-V rather than at 19 GHz-V and hence the greater contributions on the reflected down-welling atmospheric radiation.

Figure 3 shows the variation in PR and GR as a function of surface wind speed (WS) for open water, FY and MY ice surfaces. The PR shows a much larger decrease than GR associated with increasing surface wind. Surface wind-induced foam reduces the surface reflectivity and hence increases the emissivity of open

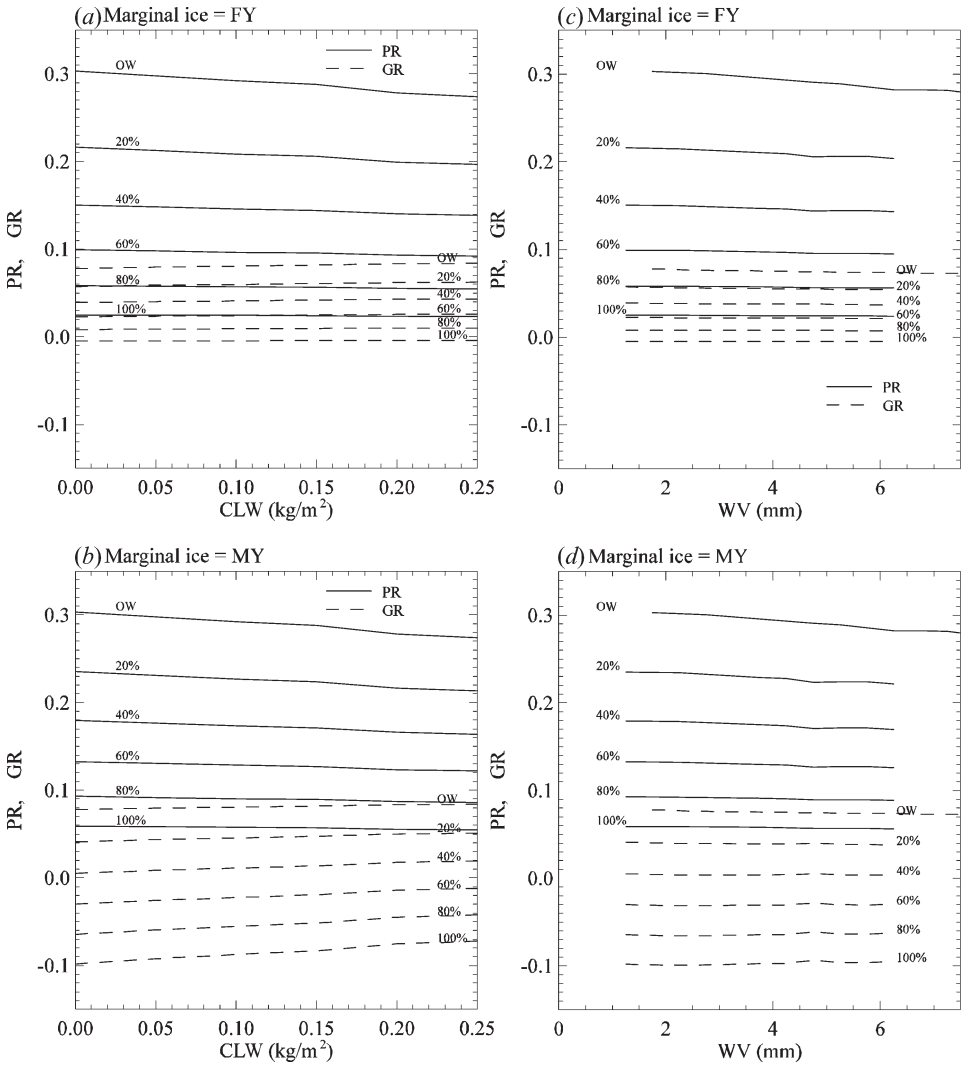

Figure 2. The polarization ratio (PR) and the spectral gradient ratio (GR) as a function of (*a*,*b*) columnar cloud liquid water (CLW) content and (*c*,*d*) columnar water vapour (WV) content at the different fractions of FY ice and MY ice at 20% intervals from open water to 100% pure ice. To discriminate the contributions from the other atmospheric parameters, the following conditions were used: WS=0 m s^{-1} and WV=1.2 mm for the signals of CLW and WS=0 m s^{-1} and CLW=0 kg m^{-2} for WV.

water. The emissivity change, however, is greater at 19 GHz-H than at 19 GHz-V, which decreases the PR with increasing WS. However, GR is relatively insensitive to WS because both channels are affected almost equally by WS change (see figure 1).

4. Synthetic retrievals

We investigate the sea ice retrieval errors due to atmospheric and surface wind effects. The NT algorithm was used for synthetic retrieval. Following Cavalieri *et al.*

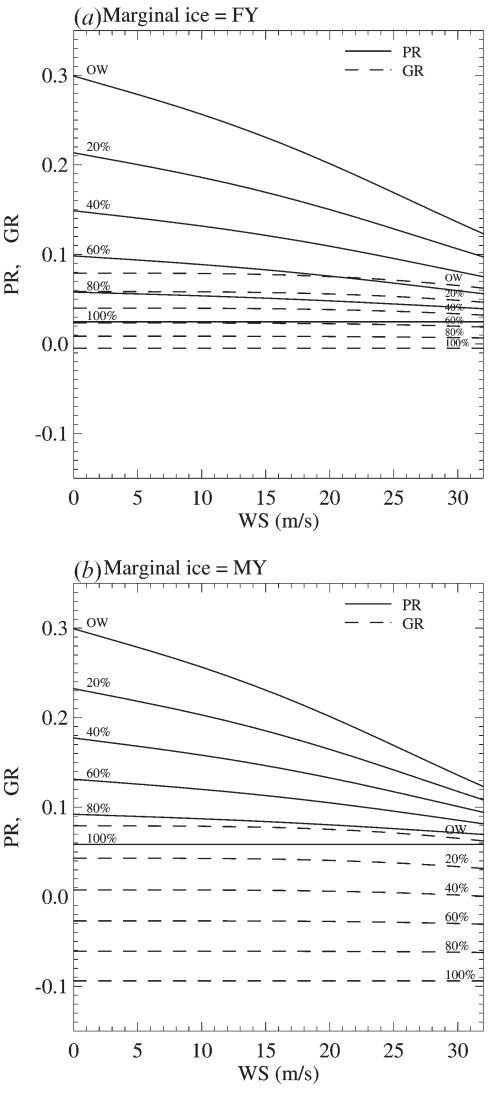

Figure 3. The polarization ratio (PR) and the spectral gradient ratio (GR) as a function of wind speed (WS) when CLW=0 kg/m^2 and WV=1.2 mm at different fractions of (*a*) FY ice and (*b*) MY ice at 20% intervals from open water to 100% pure ice.

(1984), the concentrations of FY (C_{FY}) and MY (C_{MY}) ice were computed as follows:

$$C_{FY} = (a_0 + a_1 PR + a_2 GR + a_3 PR \cdot GR)/D \quad (5)$$

$$C_{MY} = (b_0 + b_1 PR + b_2 GR + b_3 PR \cdot GR)/D \quad (6)$$

where

$$D = c_0 + c_1 PR + c_2 GR + c_3 PR \cdot GR \quad (7)$$

The coefficients a_i, b_i and c_i (i=0, 1, 2, 3) were computed from the tie points in table 1. Three surface types were considered: (a) FY ice and open water (OW), (b)

MY ice and OW, and (c) FY ice + MY ice + OW. In case (c), equal amounts of FY and MY ice were introduced. The total ice concentration (C_T) is the sum of the FY and MY ice concentrations ($C_T = C_{FY} + C_{MY}$) and $F_{FY} = F_{MY} = ½\ F_T$. Atmospheric and surface wind effects were then included by imposing variability of atmospheric and surface parameters in the range and intervals specified in section 2.

Figures 4(*a*)–4(*c*) show the scatter plots of PR and GR corresponding to the three combinations of surface types. The tie points for OW, FY and MY ice and curves of the fraction of FY and MY ice at 20% intervals are indicated. Simulation results for different fractions of sea ice are coloured differently.

In the case of FY ice retrieval, figure 4(*a*) shows that the changes of PR and GR due to WV and CLW are small whereas WS decreases PR significantly. As the dominant effect of WS is to decrease PR, the scatter points are moved outside of the retrieval triangle formed by the tie points of OW, 100% FY and 100% MY ice.

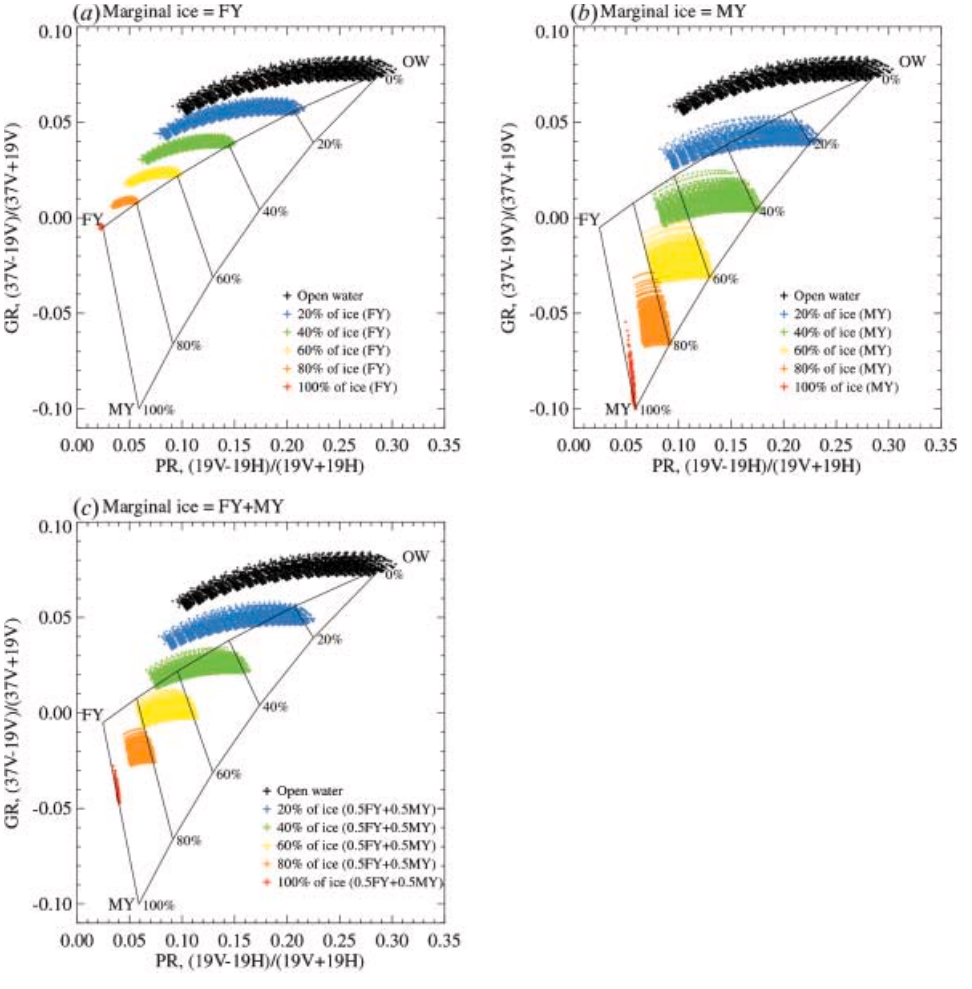

Figure 4. Scatter plots of the spectral gradient ratio (GR) *versus* the polarization ratio (PR) for the three different surface types: (*a*) open water (OW) and FY ice, (*b*) for OW and MY ice and (*c*) OW, FY and MY ices. The fractions of ices are indicated by different colours. The triangle for ice concentration retrieval is superimposed. The lines of total ice concentrations are shown in 20% intervals.

The scatter points resulting from the atmospheric effects decrease as the fraction of FY ice increases. This is because of the high contrast between the emissivity of the FY ice and OW, which overwhelms the atmospheric contributions. In the second case of MY ice, figure 4(*b*) shows that the scatter is larger than that for the corresponding FY ice. The lower contrast of emissivities between the MY ice and OW enhances the relative contribution due to atmospheric effects. The wind effects moves the scatter points towards more ice concentration areas in the retrieval triangle, hence large errors in retrieval errors are incurred. For a combination of OW, FY and MY ice (the third case, figure 4(*c*)), the scatter is somewhere in between the first and second cases.

The tie points for each surface are usually obtained from mean atmospheric profiles. Given the assumed uniform distributions (in terms of vertically integrated amount) of our simulated data, the tie points corresponding to simulated atmospheric profile data with the highest 10% of PR for OW and the lowest 10% of GR for the FY and MY ices were used. The tie point values computed herein are close to the values given in Comiso *et al.* (1997). The weather filter in Comiso *et al.* (1997) to reduce spurious sea ice concentrations over open water was included, that is for FOVs with GR values greater than 0.05, sea ice concentrations for the FOVs were set to zero.

The three cases of sea ice concentration [FY, MY and ½(FY + MY)] were used for synthetic retrievals by the NT algorithm. The retrieval uncertainty was evaluated in terms of the bias and the root mean square (RMS) error. The bias statistics is important from an operational and climatological perspective while the RMS statistics shows uncertainty of the retrieval. Table 2 summarizes the error statistics corresponding to synthetic ice concentration retrievals based on the NT algorithm for these cases. The bias and RMS error statistics are shown as a percentage relative to the true ice concentrations. The overall performance of the total sea ice concentration retrieval, as indicated by the RMS errors (the last column in the table) for all three cases, decreases as the fraction of ice increases. For ice free oceans, the atmospheric filter proposed in the NT algorithm, which has a fixed cutoff value, simply removes errors introduced by atmospheric effects. For 100% pure sea ice type coverage, the atmospheric variability does not affect the accuracy of the retrieval either. The bias statistics indicate that the inclusion of atmospheric effects tends to result in an overestimation in the retrievals of FY ice concentration for ice concentrations between 0.4 and 0.95, in terms of both absolute and relative biases. The underestimation of FY ice concentration for the cases of 0.1 FY and 0.2 FY ice concentrations is attributed to the application of the weather filter that sets some low concentration pixels to zero sea ice concentration, hence the underestimate (negative bias). For the MY ice only retrieval, MY ice concentrations are underestimated at all ranges. The RMS errors are usually higher for FY than MY ice retrieval for concentrations below 0.6, but are lower for higher sea ice concentrations.

We next examined the relative sensitivity of atmospheric parameters and surface wind on sea ice concentration estimates. Figures 5(*a*) and 5(*c*) show the retrieved FY ice concentrations (C_{FY}) as a function of CLW for a calm sea (WS = 0 m s^{-1}) and as a function of WS for a non-cloudy (CLW = 0) atmosphere. Figures 5(*b*) and 5(*d*) show similar retrievals for MY ice. In all the cases, WV is fixed at 2 mm. The FY ice concentrations are overestimated in the presence of CLW and SW (the curves slope upwards) and the MY ice underestimated (curves slopes downwards). If we compare

Table 2. Statistics corresponding to synthetic sea ice concentration retrievals for various fractions of ice and surface types. The bias and root mean squared (RMS) error statistics are presented as a percentage relative to the true sea ice concentration. The FY + MY category indicates equal concentrations of first-year (FY) and multi-year (MY) ice. For example, for 0.2 sea ice concentration, the FY + MY case indicates 10% FY and 10% MY sea ice concentration.

	Retrieved sea ice concentration			Bias (%)			RMS error (%)		
True sea ice concentration	FY	MY	Total	FY	MY	Total	FY	MY	Total
FY=0.1	0.026	0.000	0.026	−73.70	–	−73.70	162.68	–	162.68
MY=0.1	0.123	0.000	0.123	–	−100.00	22.82	–	100.00	259.48
FY=0.05, MY=0.05	0.074	0.000	0.074	48.99	−100.00	−25.51	453.60	100.00	226.90
FY=0.2	0.174	0.000	0.174	−13.02	–	−13.02	164.10	–	164.10
MY=0.2	0.305	0.064	0.369	–	−67.94	84.46	–	75.93	113.19
FY=0.1, MY=0.1	0.335	0.015	0.350	234.68	−84.61	75.03	351.70	90.18	146.94
FY=0.4	0.635	0.000	0.635	58.73	–	58.79	70.34	–	70.34
MY=0.4	0.249	0.271	0.519	–	−32.30	29.85	–	37.60	37.49
FY=0.2, MY=0.2	0.442	0.084	0.526	120.88	−58.06	31.41	143.27	66.05	39.82
FY=0.6	0.762	0.000	0.763	27.08	–	27.11	32.18	–	32.18
MY=0.6	0.190	0.490	0.681	–	−18.25	13.43	–	21.77	16.97
FY=0.3, MY=0.3	0.477	0.207	0.683	58.84	−31.07	13.88	68.72	36.03	17.34
FY=0.8	0.888	0.000	0.888	10.94	–	10.95	12.83	–	12.83
MY=0.8	0.134	0.705	0.839	–	−11.90	4.84	–	14.97	6.36
FY=0.4, MY=0.4	0.511	0.331	0.842	27.78	−17.25	5.27	32.04	20.67	6.63
FY=0.9	0.949	0.000	0.949	5.43	–	5.43	6.26	–	6.26
MY=0.9	0.107	0.810	0.917	–	−10.01	1.84	–	13.04	2.76
FY=0.45, MY=0.45	0.528	0.392	0.920	17.43	−12.96	2.23	20.37	16.13	2.93
FY=0.95	0.979	0.000	0.979	3.04	–	3.04	3.43	–	3.43
MY=0.95	0.093	0.862	0.955	–	−9.27	0.53	–	12.29	1.43
FY=0.475, MY=0.475	0.537	0.422	0.959	13.07	−11.18	0.94	15.79	14.39	1.39
FY=1.0	1.00	0.000	1.000	0.00	–	0.00	0.00	–	0.00
MY=1.0	0.080	0.913	0.993	–	−8.70	−0.75	–	11.68	1.17
FY=0.5, MY=0.5	0.546	0.451	0.997	9.18	−9.76	−0.29	12.13	12.90	0.55

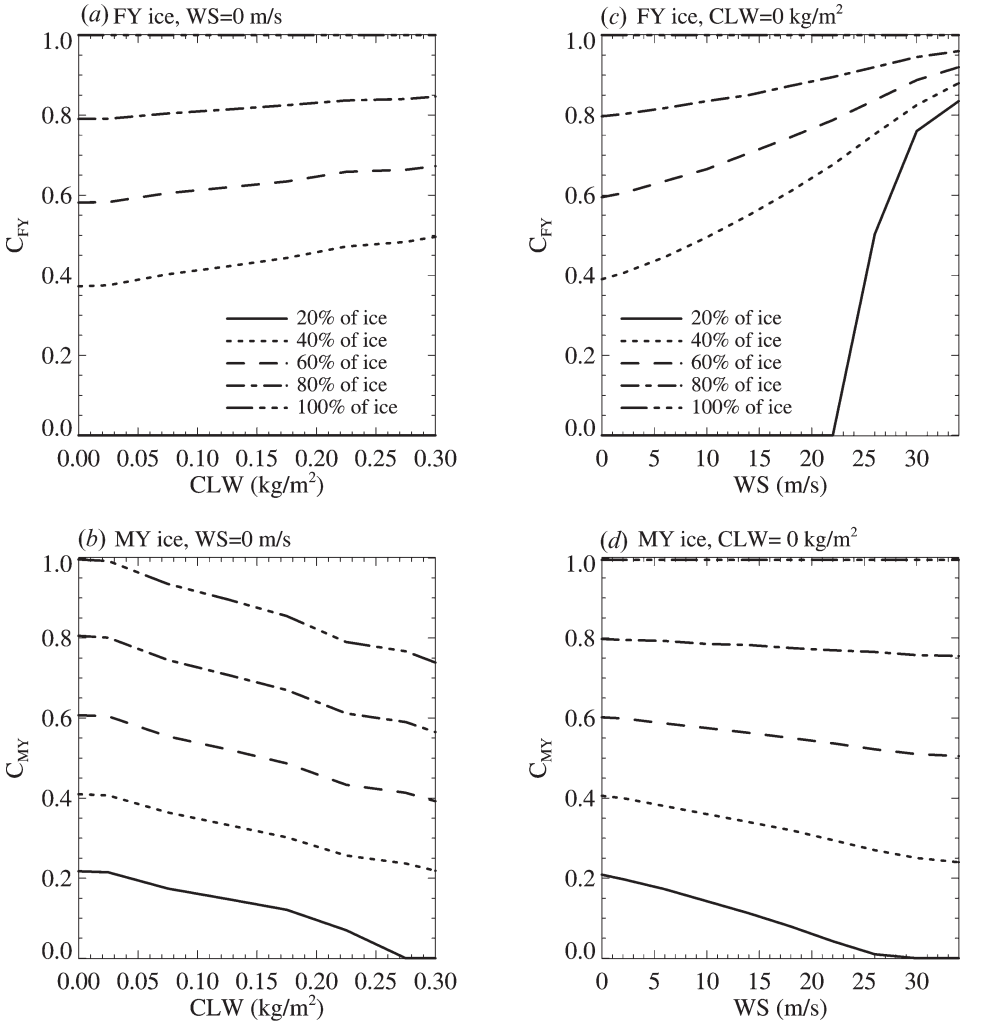

Figure 5. FY and MY ice concentrations (C_{FY}, C_{MY}) for each surface type as a function of (*a*,*b*) columnar cloud liquid water content (CLW) when surface wind speed (WS) is $0\,m\,s^{-1}$ and as a function of (*c*,*d*) WS when CLW is $0\,kg\,m^{-2}$. The columnar water vapour (WV) content is fixed at 2 mm for both the cases.

the slopes of the sea ice concentration curves, it can be seen that the FY overestimates are more sensitive to WS. The underestimates for MY ice are less dramatic for WS than for CLW and show a strong dependency on sea ice concentration (more sensitive to the low sea ice concentrations). It can thus be inferred that the surface wind effect on the retrieval error is greater for FY ice than that due to CLW within the typical ranges of these parameters. The weather filter (GR$<$0.05) automatically sets FY concentrations of 20% or less to 0% (figure 5(*a*)), but at WS greater than about $22\,m\,s^{-1}$, the radiometric signatures are increased beyond the limit of the weather filter, resulting in the huge overestimation of the FY ice fraction (figure 5(*c*)). For MY ice, the underestimate is more sensitive to CLW than WS.

Figure 6 shows the retrieved total ice concentrations (C_T) as a function of CLW and WS for different ice fractions and surface types. The left columns

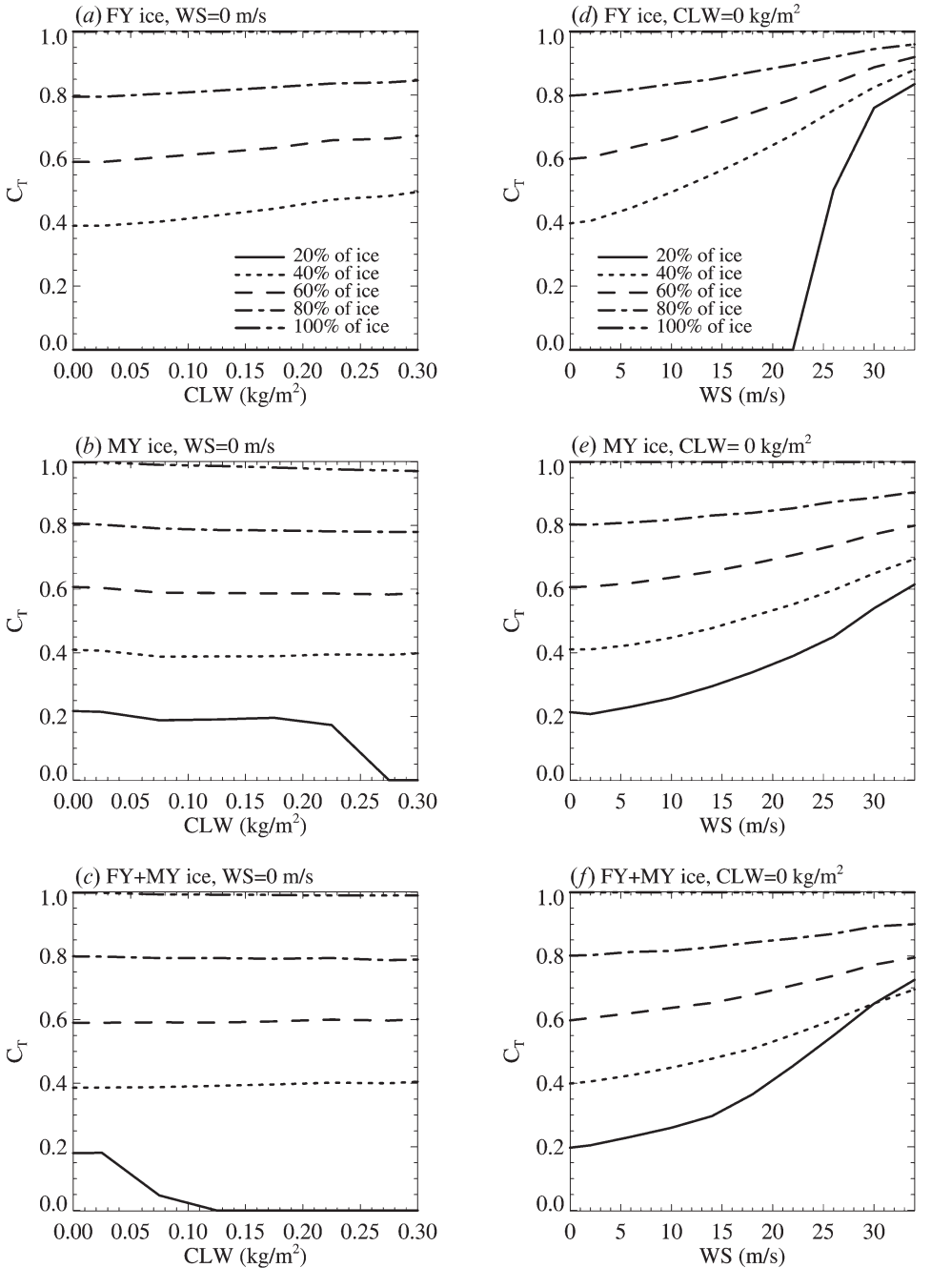

Figure 6. Same as figure 5 but for total ice concentrations ($C_T = C_{FY} + C_{MY}$) for the three different surface types.

(figures 6(*a*)–6(*c*)) show retrieved C_T as a function of CLW when WS is zero (calm surface). The right columns (figures 6(*d*)–6(*f*)) show retrieved C_T as a function of WS when CLW is zero, that is a clear atmosphere. The WV is again fixed at 2 mm. For FY ice and WS = 0 m s^{-1} (figure 6(*a*)), the retrieved sea ice concentration increases

with increasing CLW for ice concentrations between 0.4 and 0.8, but does not affect the estimates for 100% of ice. At 0.2 FY ice concentration, no sea ice is retrieved, mainly because of the use of the weather filter ($C_T=0$ if GR$>$0.05). For MY ice (figure 6(*b*)) and FY + MY ice (figure 6(*c*)), the retrieval errors are small. Due to the application of the GR cutoff value, there is also a notable underestimation of C_T when CLW is $>0.23\,\mathrm{kg\,m^{-2}}$ for MY ice and no sea ice is retrieved for CLW$>0.12\,\mathrm{kg\,m^{-2}}$ for the FY + MY ice combination. The variability of WV appears to affect the retrievals in a similar way as found in the CLW case, but its effect is much less pronounced than that of CLW (results not shown here). Figures 6(*d*)–6(*f*) show the effect of surface wind on sea ice concentration retrievals. In the presence of high wind, more sea ice is retrieved for ice concentration in excess of 0.2. This is probably because of the reduced polarization resulting from the wind-driven foam, which covers the ocean surface in a way independent of polarization. Note also that no sea ice is retrieved when the ice fraction is less than 0.2 and WS is less than $22\,\mathrm{m\,s^{-1}}$ (figure 6(*d*)). This is again attributed to the weather filter. At high wind speed (WS$>22\,\mathrm{m\,s^{-1}}$), the total sea ice concentration is substantially overestimated. If we compare the left and the right columns of figure 6, it can be seen that the sea ice retrieval is more sensitive to WS than CLW (or WV) within the range of variabilities of these parameters.

5. Summary and discussion

In this study, we performed a simulation study to examine the errors due to atmospheric effects and surface wind in microwave retrieval of sea ice concentrations. Three surface types were considered, OW, FY and MY ice, and their combinations. Atmospheric profiles of WV and CLW typical of the Arctic summer were generated with variable surface wind and surface types. A plane parallel Eddington radiative transfer model was used to compute brightness temperatures at the SSM/I channels based on the simulated data. The dependence of the surface emissivity of the open ocean on surface wind was also included. Two models of surface emissivity of open water were considered, the Wilheit and Wentz models. Our results show that the difference between the models is small and only the results using the Wilheit model are presented. The Wilheit model can be easily adapted for other sensors, such as the AMSR onboard NASA's Aqua satellite. The NT sea ice algorithm was used for synthetic retrievals. This study may be extended to include other microwave retrieval algorithms.

The NT algorithm uses PR and GR for retrievals. PR is decreased in the presence of atmospheric and surface contributions (CLW, WV and surface wind), but the effect of depolarization due to the wind-driven ocean foam has a pronounced effect on the decrease of PR for both of FY and MY ice surfaces. Increases in CLW tend to increase GR whereas increases in WV and surface wind slightly reduce GR. Synthetic retrievals using the NT algorithm based on the simulated data show overestimations of FY ice concentration due to the atmospheric water and greater overestimation due to surface wind. MY ice concentrations are underestimated. The overestimate of FY and underestimate for MY ice concentrations are consistent with previous work (Maslanik 1992, Oelke 1997). This study, however, demonstrates the strong effect of surface wind in contributing to the retrieval error of FY and total ice concentrations, especially over marginal ice areas, which has only received little attention in previous studies. This is significant because the position of the sea ice edge is strongly affected by surface wind convergence or divergence

(Cahalan and Chiu 1986). Moreover, our sensitivity study shows that the errors due to surface wind depend nonlinearly on sea ice concentration and surface wind shows a stronger effect on retrieval than CLW. These results can be compared to those of Maslanik (1992), who showed that the error in ice concentration estimates is linearly related to surface wind and is smaller than the effect due to liquid water.

Our results also show that the NT retrievals for pure open ocean and 100% ice surfaces are relatively unaffected by the atmospheric conditions. The NT weather filter only masked out pixels at low ice concentrations and open water, and no filtering takes place at higher concentrations. This procedure, however, also masks out surfaces with small sea ice concentration, thus giving rise to a small negative bias for surfaces with small sea ice concentrations (0.2).

In computing our ensemble, the vertical distributions of each parameter were not uniform but their integrated amounts (columnar CLW content and columnar WV content) and surface wind were assumed to have a uniform distribution (at discrete intervals). This assumption was used for its simplicity in our study because our aim was to understand the impact of these variables on the microwave signature for retrieval. However, the atmospheric variables have different distributions temporally and regionally. In addition, they are correlated. For example, in frontal zones, strong surface wind tends to be associated with increase cloudiness and water vapour. To compute the bias and RMS statistics that are appropriate for the specific period and region, more realistic distributions of the atmospheric variables must be used (e.g. Oelke 1997). Other major uncertainties, such as the ice surface temperature, especially for MY ice, and snow conditions, will also affect microwave retrieval. Sea ice parameters, such as sea ice surface temperature, recently derived from the Moderate Resolution Interferometer Spectroradiometer (MODIS; Hall *et al.* 2004) and atmospheric profiles derived from the Atmospheric Infrared Sounder/Atmospheric Microwave Sounding Unit/Humidity Sounding from Brazil (AIRS/AMSU/HSB) package (Aunmann *et al.* 2003) will provide additional information to narrow down the errors in microwave sea ice retrieval. The additional atmospheric and surface information can be incorporated into our simulation models and radiative transfer computations to aid sea ice analysts in the interpretation of sea ice products from microwave sensors.

Acknowledgements

L.C. is supported by a Joint Navy/NOAA National Ice Center contract to the George Mason University Center for Earth Observing and Space Research through a cooperative agreement between the two institutions.

References

Anderson, S., Tonboe, R., Kaleschke, L., Heygster, G. and Pederson, L.T., 2007, Intercomparison of passive microwave sea ice concentration retrievals over the high-concentration Arctic sea ice. *Journal of Geophysical Research*, **112**, pp. 4693–4700.

Aunmann, H.H., Chahine, M.T., Gautier, C., Goldberg, M.D., Kalnay, E., McMillin, L.M., Revercomb, H., Resenkranz, P.W., Smith, W.L., Staelin, D.H., Strow, L.L. and Susskind, J., 2003, AIRS/AMSU/HSB on the Aqua Mission: design, science objectives, data products, and processing systems. *IEEE Transactions on Geoscience and Remote Sensing*, **41**, pp. 253–264.

Cahalan, R. and Chiu, L.S., 1986, Large-scale short-period atmosphere–sea ice interaction. *Journal of Geophysical Research*, **91**, pp. 10709–10717.

CAVALIERI, D., GLOERSEN, J.P. and CAMPBELL, W.J., 1984, Determination of sea ice parameters with the NIMBUS 7 SMMR. *Journal of Geophysical Research*, **89**, pp. 5355–5369.

COMISO, J.C., CAVALIERI, D.J., PARKINSON, C.L. and GLOERSEN, P., 1997, Passive microwave algorithms for sea ice concentration: a comparison of two techniques. *Remote Sensing of Environment*, **60**, pp. 357–384.

COX, C. and MUNK, W., 1955, Some problems in optical oceanography. *Journal of Marine Research*, **4**, pp. 63–78.

GLOERSEN, P., CAMPBELL, W., CAVALIERI, D., COMISO, J., PARKINSON, C. and ZWALLY, H.J., 1992, Arctic and Antarctic sea ice, 1978–1987: satellite passive microwave observations and analysis. NASA Special Publication No. 511 (Washington, D.C.: NASA).

HALL, D., KEY, J.R., CASEY, K.A., RIGGS, G.A. and CAVALIERI, D.J., 2004, Sea ice surface temperature product from MODIS. *IEEE Transactions on Geoscience and Remote Sensing*, **42**, pp. 1076–1087.

JACKSON, J.D., 1962, *Classical Electrodynamics*. (New York: John Wiley and Sons).

JOHANNESSEN, O.M., SHALINA, E.V. and MILES, M.W., 1999, Satellite evidence for an Arctic sea ice cover in transformation. *Science*, **286**, pp. 1937–1939.

KUMMEROW, C., 1993, On the accuracy of the Eddington approximation for radiative transfer in the microwave frequencies. *Journal of Geophysical Research*, **98**, pp. 2757–2765.

MARKUS, T. and CAVALIERI, D.J., 2000, An enhancement of the NASA team sea ice algorithm. *IEEE Transactions on Geoscience and Remote Sensing*, **38**, pp. 1387–1398.

MARKUS, T. and DOKKEN, S.T., 2002, Evaluation of late summer passive microwave Arctic sea ice retrievals. *IEEE Transactions on Geoscience and Remote Sensing*, **40**, pp. 348–356.

MASLANIK, J.A., 1992, Effects of weather on the retrieval of sea ice concentration and ice type from passive microwave data. *International Journal of Remote Sensing*, **13**, pp. 37–54.

MEIER, W., MARQUIS, M., KAMINSKI, M. and WEAVER, R., 2004, NASA EOS sensors demonstrate potential for multiparameter studies of arctic sea ice. *Eos Transactions AGU*, **85**, pp. 481–488.

MEIER, W., STROEVE, J., FETTERER, F. and KNOWLES, K., 2005, Reductions in Arctic sea ice cover no longer limited to summer. *Eos Transactions* AGU, **86**, pp. 326–327.

MITNIK, M.L. and MITNIK, L.M., 2004, Atmospheric parameters over the marginal ice zone retrieval from AMSR/AMSR E data. *Gayana*, **68**, pp. 396–401.

OELKE, C., 1997, Atmospheric signatures in sea-ice concentration estimates from passive microwaves: modelled and observed. *International Journal of Remote Sensing*, **18**, pp. 1113–1136.

PARKINSON, C.L., CAVALIERI, D., GLOERSEN, P., ZWALLY, H.J. and COMISO, J., 1999, Arctic sea ice extents, area, and trends, 1978–1996. *Journal of Geophysical Research*, **104**, pp. 20387–20856.

SVENDSEN, S., KLOSTER, K., JOHANNESSEN, O., JOHANNESSEN, J., CAMPBELL, W., GLOERSEN, P., CAVALIERI, F.D. and MATZLER, C., 1983, Norwegian remote sensing experiment: evaluation of the NIMBUS 7 Scanning Microwave Radiometer for sea ice research. *Journal of Geophysical Research*, **88**, pp. 2718–2791.

WENTZ, F.J., 1992, Measurement of oceanic wind vector using satellite microwave radiometers. *IEEE Transactions on Geoscience and Remote Sensing*, **30**, pp. 962–972.

WILHEIT, T.T., 1979, A model for the microwave emissivity of the ocean's surface as a function of wind speed. *IEEE Transactions on Geoscience and Electronics*, **17**, pp. 244–249.